Osteopontin–metallothionein I/II interactions in experimental autoimmununе encephalomyelitis

Jakovac, Hrvoje; Grubić Kezele, Tanja; Šućurović, Sandra; Mulac-Jeričević, Biserka; Radošević-Stašić, Biserka

Source / Izvornik: **Neuroscience, 2017, 350, 133 - 145**

Journal article, Published version
Rad u časopisu, Objavljena verzija rada (izdavačev PDF)

https://doi.org/10.1016/j.neuroscience.2017.03.020

Permanent link / Trajna poveznica: https://urn.nsk.hr/urn:nbn:hr:184:803749

Neuroscience 350 (2017) 133–145

OSTEOPONTIN–METALLOTHIONEIN I/II INTERACTIONS IN EXPERIMENTAL AUTOIMMUNUNE ENCEPHALOMYELITIS

HRVOJE JAKOVAC,[†] TANJA GRUBIĆ KEZELE[†] SANDRA ŠUĆUROVIĆ BISERKA MULAC-JERIČEVIĆ AND BISERKA RADOŠEVIĆ-STAŠIĆ[*]

Department of Physiology and Immunology, Medical Faculty, University of Rijeka, B. Branchetta 22, 51 000 Rijeka, Croatia

Abstract—Osteopontin (OPN), an extracellular matrix (ECM) glyco-phosphoprotein, plays an important role in autoimmune-mediated demyelinating diseases, including multiple sclerosis and experimental autoimmune encephalomyelitis (EAE). As an integrin and CD44 binding protein it participates in bidirectional communication between the ECM and target cells and affects transduction pathways that maintain neuronal and immune cell homeostasis. Its biological activity is also heavily influenced by microenvironment, which stimulates the cleavage of OPN and changes its functions. In this study we estimated the expression profile of OPN in neural tissues of DA rats during the first relapse of chronic relapsing EAE and investigated the relationship of OPN to metallothionein I + II (MTs), which play pivotal role in zinc-related cell homeostasis and in protection of CNS against cytokine-induced injury. The data showed that in EAE rats OPN mRNA and protein levels increased concurrently with the transcription of MTs and that within the spinal cord (SC) lysates EAE-afflicted rats had a higher content of OPN fragments of low molecular weight than untreated and CFA-treated rats. The expression of OPN and MTs was upregulated on ependymal, lymphoid and astroglial cells and on multiple αvβ3+ neurons in SC and in the brain (cortex, white matter, hippocampus, and cerebellum). Besides, multiple cells co-expressed OPN and MTs. Granular OPN signals were detected in secretory vesicles of Golgy (αvβ3 neurons) and in patches adjacent to the plasma membrane (subventricular zone). The findings imply that in demyelinating lesions are generated proteolytic OPN fragments and that OPN/MT interactions contribute to tissue remodeling during an autoimmune attack.

Key words: αvβ3 integrin receptor, experimental autoimmune encephalomyelitis, extracellular matrix, metallothioneins, neuroprotection, osteopontin cleavage.

*Corresponding author. Fax: +385-51-675-699.
E-mail address: biserkars@medri.uniri.hr (B. Radošević-Stašić).
[†] Equally contributed to this study.

Abbreviations: ALS, amyotrophic lateral sclerosis; CFA, complete Freund's adjuvant; EAE, encephalomyelitis; ECM, extracellular matrix; EDTA, ethylenediaminetetraacetic acid; HEPES, 4-(2-hydroxyethyl)-1-piperazineethanesulfonic acid; IL-10, interleukin-10; MS, multiple sclerosis; MT, metallothionein; OPN, osteopontin; PCNA, proliferating cellular nuclear antigen.

INTRODUCTION

Osteopontin (OPN), known also as secreted phosphoprotein 1 and early T lymphocyte activation 1 (ETA-1) is an extracellular matrix (ECM) protein, which belongs to a family of small integrin-binding ligand N-linked glycoproteins (SIBLINGs). It was first described by Senger and coauthors as a 60-kDa phosphoprotein, secreted from transformed mammalian cells (Senger et al., 1979). Lately, it was identified in osteoblasts and bone calcified matrix, but today it is known that OPN acts as a pleiotropic cytokine, which in various cells affects multiple physiological and pathological processes (Ashkar et al., 2000; Fisher et al., 2001; Bellachene, 2008).

Current knowledge also shows that functional properties of SIBLINGs depend on functions of extracellular proteases and cellular uptake of ECM proteins or their proteolysed fragments, as well as on processes that regulate their trafficking into the secretory and the endo/lysosomal degradation pathways inside the cells (Bellachene, 2008; Hellewell and Adams, 2015). Importantly, some ECM components after proteolysis may exhibit differential biological activities owing to the removal of functional domains or exposure of cryptic binding sites (Fedarko et al., 2004).

In this context it is known that full length OPN contains an arginine-glycine-aspartate (RGD) motif at NH2-terminal fragment and a protease-hypersensitive cleavage site that separates the integrin-binding site from the C-terminal fragments of OPN containing CD44 binding domains (reviewed by (Okamoto, 2007; Scatena et al., 2007). The RGD sequence, which is 100% conserved between species, acts as a major binding site for αv/β3, αv/β1, α5/β1, α8/β1, and αv/β5 integrins (Ashkar et al., 2000; Denhardt et al., 2001). Cleavage by thrombin at Arg168–Ser169 exposes a serine-valine valine-tyro sine-glutamate-leucine-arginine (SVVYGLR) domain (human) or SLAYGLR domain (mouse and rat). It is cryptic in intact OPN, but after cleavage with thrombin it binds α9/β1 and α4/β1 integrins that are the main adhesion molecules involved in lymphocyte transmigration to the brain (Smith et al., 1996; Yokosaki et al., 1999; Green et al., 2001; Boggio et al., 2016). Importantly, additional cleavage of OPN within the SVVYGLR site may be induced by several MMPs, including MMP2, MMP3, MMP7, MMP9, and MMP12 (Agnihotri et al., 2001; Gao

http://dx.doi.org/10.1016/j.neuroscience.2017.03.020

et al., 2004; Hou et al., 2004; Goncalves DaSilva et al., 2010). These new MMP-cleaved OPN fragments may exhibit reduced ability to bind α4/α9 integrins (Yokosaki et al., 2005), but also the greater adhesive and migratory activities than full-length OPN (Gao et al., 2004).

Through sequences in C-terminal fragment OPN interacts also with CD44v3–v6 splice variants in an RGD independent manner (Weber et al., 1999) and participates in immune regulation (Guan et al., 2011) and in tumorigenesis (Teramoto et al., 2004). Besides, OPN molecule contains heparin binding, hydroxyapatitite and calcium binding regions and domains responsible for transglutamination, as well as multiple Ser and Thr phosphorylation sites and sites for N- and O-linked glycosylation (Okamoto, 2007; Scatena et al., 2007). Furthermore, along to its classically secreted form (s-OPN) OPN also exists in an intracellular form (i-OPN) (Shinohara et al., 2008a; Cantor and Shinohara, 2009; Hellewell and Adams, 2015; Rittling and Singh, 2015). It may be generated from the same mRNA as s-OPN by alternative translation of a non-AUG site downstream of the canonical AUG sequence and accompanied by deletion of the N-terminal 16-aa signal sequence that targets nascent protein to secretory vesicles (Shinohara et al., 2008b). Reports show that this form of OPN is a critical regulator for Toll like receptor-9 (TLR-9), TLR-7-dependent interferon-alpha (IFN-alpha) expression by plasmacytoid dendritic cells (DCs) and TH17 development (Shinohara et al., 2008a; Cantor and Shinohara, 2009; Morimoto et al., 2010; Inoue and Shinohara, 2011; Hellewell and Adams, 2015).

Collectively, these data emphasize that pleiotropic functions of OPN depend on discrete changes in domains, on generation of its active cleaved products and on processes of posttranslational modifications, such as phosphorylation, glycosylation and sulphation that may generate different functional forms of OPN.

As a multi-faceted molecule OPN plays an important role also in neurodegenerative diseases, such as Parkinson's and Alzheimer's disease, as well as in multiple sclerosis (MS) and its animal model experimental autoimmune encephalomyelitis (EAE) (Steinman, 2009; Braitch and Constantinescu, 2010; Carecchio and Comi, 2011; Niino and Kikuchi, 2011). In these conditions OPN is mainly considered an inflammatory molecule, but since in some contexts OPN may function as a neuroprotectant, its ambiguous and "double-edged" sword activities have been often emphasized (Carecchio and Comi, 2011).

The detrimental role of OPN in MS and EAE was first reported by Chabas and colleagues (2001) who showed that OPN transcript was abundant in plaques dissected from brains of patients with MS and within SC tissue of rats paralyzed by EAE, as well as that OPN−/− mice were resistant to progressive EAE. They also found that myelin-reactive T cells in OPN−/− mice produced more interleukin-10 (IL-10) and less interferon-γ than in OPN +/+ mice, proposing that OPN might regulate T helper cell-1 (TH1)-mediated autoimmune diseases (Chabas et al., 2001). The data were confirmed by findings that OPN-deficient mice had attenuated EAE and decreased inflammatory infiltration and demyelination in the spinal cords (Jansson et al., 2002), by data showing that treatment of EAE mice with recombinant (r) OPN might exacerbate the disease in OPN-deficient mice and trigger neurological relapse by inhibiting apoptosis of autoreactive immune cells (Hur et al., 2007), as well as by findings that anti-OPN treatment might reduce clinical severity of EAE and IL-17 production (Murugaiyan et al., 2008).

It should be also emphasized that the expression profile of OPN and its receptors show, time- and cell-dependent patterns (Kang et al., 2008), as well as that OPN functions strictly depend on microenvironment in which thrombin (Boggio et al., 2016), or different MMPs (Agnihotri et al., 2001; Gao et al., 2004; Hou et al., 2004; Goncalves DaSilva et al., 2010) contribute to proteolytic cleavage of OPN and generation of OPN fragments with distinct functions.

In this context, it has been shown that the RGD-binding domain of OPN might also enhance the survival of tyrosine hydroxylase (TH)-positive cells in rat substantia nigra against toxic insults (Iczkiewicz et al., 2010), as well as that OPN in distinct conditions might have not only detrimental, but also a protective properties (Braitch and Constantinescu, 2010; Carecchio and Comi, 2011; Brown, 2012), participating in processes of remyelination (Zhao et al., 2008), in regeneration of peripheral motor axons (Wright et al., 2014), hippocampal neurons (Plantman, 2012) and nigral cells (Iczkiewicz et al., 2006).

In the present study, we examined the possibility that in the remodeling processes that take part in EAE OPN co-operates with metallothioneins (MTs), since this family of phylogenetically highly conserved proteins generally provide cytoprotective action against oxidative injury, DNA damage and apoptosis (Miles et al., 2000; Coyle et al., 2002). As metal-binding and cysteine-rich proteins they participate in maintenance of Zn and Cu homeostasis, in protection against cytotoxicity of toxic metals, as well as in regulation of basic cellular processes, such as gene expression, apoptosis, proliferation, and differentiation. Furthermore, acting through thiol groups, MTs ensure the protection against various types of injuries resulting from reactive oxygen (ROS) or nitrogen species (RNS), providing anti-inflammatory and immunoregulatory functions (Andrews, 2000; Mocchegiani et al., 2000; Rink and Haase, 2007; Inoue et al., 2009; Isani and Carpene, 2014; Ling et al., 2016). Importantly, it is generally accepted that MT isoforms MT-I + II, have marked neuroprotective capacities (Penkowa, 2006; Pedersen et al., 2009; Manso et al., 2011), and an impressive regulatory effect in demyelinating and inflammatory disease, such as MS and EAE (Penkowa et al., 2003; Penkowa and Hidalgo, 2003).

EXPERIMENTAL PROCEDURES

Experimental animals

Experiments were performed on male Dark Agouti (DA) rats, aged 2–3 months. They were housed under standard conditions of light, temperature and humidity with unlimited access to food and water. Experimental

procedures involving animals complied with Croatian laws and rules (NN 135/06; NN 37/13; NN 125/13; NN 055/2013) and with the guidelines set by European Community Council Directive (86/609/EEC). Experimental protocol was approved by the Ethics Committee of the University of Rijeka.

EAE induction and evaluation

Induction of chronic relapsing (CR)-EAE was performed in male DA rats by bovine brain white matter homogenate emulsion (BBH) in the complete Freund's adjuvant (CFA) (Sigma, St. Louis, Mo., USA), as previously described (Jakovac et al., 2011). To each animal 2 × 0.1 mL emulsion was injected subcutaneously in each hind footpad. Control group was injected with the same dose of CFA. The evaluation of the clinical course was assessed daily using the following criteria: 0 – no symptoms; 1 – flaccid paralysis of tail; 2 – hind legs paresis; 3 – hind legs paralysis with incontinence and 4 – death of the animal.

Tissue preparation for paraffin slices

Animals with clinical score 3 (hind legs paralysis with incontinence) were sacrificed by exsanguination on day 13 or 14 after immunization. The exsanguination was done in deep anesthesia, induced by combination of Ketamine (80 mg/kg) and Xylasine (5 mg/kg), given by intraperitoneal (i.p.) injection, according to the guidance of European Community Council Directive (86/609/EEC) and recommendation of National Centre for the Replacement, Refinement and Reduction of Animals in Research (www.nc3rs.org.uk). The tissue samples of the lumbar spinal cord and the brain were rapidly removed from nine rats and fixed in 4% buffered paraformaldehyde (Sigma, Aldrich, St. Lois, MD, USA) solution during 24 h. Tissue was then embedded in paraffin wax and sections were cut at 4 μm using HM 340E microtome (Microtom, Germany). Heat induced epitope retrieval was done prior to staining procedure by heating tissue slides in boiled citrate buffer pH 6.0 four times, each 5 min, using a microwave steamer.

Immunohistochemistry

Immunohistochemical labeling of MT I + II proteins was performed on paraffin embedded tissues using DAKO EnVision + System, Peroxidase (DAB) kit according to the manufacturer's instructions (DAKO Cytomation, Glostrup, Danmark), as previously described (Jakovac et al., 2011). Briefly, after washing and blocking non-specific binding and endogenous peroxidase activity mouse monoclonal anti-MT I + II IgG_1 antibody (clone E9; Dako Cytomation, Glostrup, Denmark; 1:50 with 1% BSA in PBS) were added to tissue samples and incubated overnight at 4 °C in a humid environment, followed by 45 min incubation with peroxidase labeled polymer conjugated to goat anti-mouse immunoglobulins containing carrier protein linked to Fc fragments to prevent nonspecific binding. The immunoreaction product was visualized by adding substrate-chromogen (DAB) solution.

For immunohistochemical analysis of OPN expression deparaffinized tissue sections were incubated with 1% BSA in PBS for one hour at room temperature to block non-specific binding. Immediately afterward, incubation with goat polyclonal anti-OPN IgG antibody, which recognizes all OPN isoforms (R&D, Minneapolis, MN, USA, 1:200 with 1% BSA in PBS) was performed overnight at 4 °C in a humid environment. After washing, tissues were incubated with secondary HRP horse anti-goat IgG antibodies (Vector Laboratories, Burlingame, CA, USA, 1:400 with 1% BSA in PBS) for one hour at room temperature in a humid environment. Immunoreactivity was visualized using DAB solution.

All tissues were counterstained with hematoxylin, dehydrated through gradient of ethanol, mounted using Entelan (Sigma-Aldrich, St. Lois, MO, USA) and examined with Olympus BX51 microscope (Olympus, Tokyo, Japan). The specificity of staining was confirmed by negative controls. For OPN-immunostaining, tissue samples were treated with an identical procedure under the same conditions, but with the omission of polyclonal primary antibodies. For MT-I + II-immunostaining, tissue samples were incubated with isotype-matched irrelevant antibodies (mouse IgG1 immunoglobulin, clone DAK-G01; Dako Cytomation, Glostrup, Danmark).

Immunofluorescence

Immunofluorescence labeling was also performed on paraffin-embedded tissue sections. Nonspecific binding was blocked by one-hour incubation with 1% BSA in PBS containing 0.001% NaN_3 at room temperature. The following primary antibodies were used: goat anti-OPN IgG (R&D, Minneapolis, MN, USA, 1:200), rabbit anti-Integrin beta 3 IgG (Abcam, Cambridge, UK, 1:100), rat anti-CD44 as a supernatant from rat hybridoma, clone IM7 (own production), mouse anti-MT-I + II IgG_1 (clone E9; Dako Cytomation, Glostrup, Denmark; 1:50), rabbit anti-GFAP IgG (Abcam, Cambridge, UK, 1:5000), rabbit anti-NeuN IgG (Abcam, Cambridge, UK, 1:100), mouse anti-GM130 IgG_1 (clone 35, BD Bioscience, San Jose, CA, SAD, 1:100) and mouse anti-proliferating cellular nuclear antigen (PCNA) IgG2a (Abcam, Cambridge, UK, 1:100). Primary antibodies were diluted in blocking solution and incubated with tissue sections overnight at 4 °C in a humid environment. To visualize immunocomplexes, the following secondary antibodies were used: Alexa Fluor donkey anti-rabbit IgG 594 nm (Molecular Probes, Carlsbad, CA, USA, 1:500), Alexa Fluor donkey anti-goat IgG 488 nm (Molecular Probes, Carlsbad, CA, USA, 1:300), Alexa Fluor donkey anti-rat IgG 594 nm (Molecular Probes, Carlsbad, CA, USA, 1:500), Alexa Fluor goat anti-mouse IgG1 555 nm (Molecular Probes, Carlsbad, CA, USA, 1:500) and Alexa Fluor goat anti-mouse IgG 488 nm Molecular Probes, Carlsbad, CA, USA, 1:300). Secondary antibodies were diluted in blocking solution and incubated with tissue sections in the dark for 1 h at room temperature in a humid environment. Nuclei were visualized with 4′,6-diamidino-2-phenylindole, dihydrochloride (DAPI, Molecular Probes, Carlsbad, CA, USA). The specificity of the reaction was confirmed by

omission of primary antibodies on slides treated with an identical procedure under the same conditions.

Images were captured on Olympus imaging system BX51 equipped with DP71CCD camera (Olympus, Tokyo, Japan) and CellF imaging software was used.

Western blot analyses

Spinal cords were collected from rats treated with BBH + CFA ($N = 3$), with CFA ($N = 3$) and from untreated ($N = 3$) rats. Samples were snap-frozen in liquid nitrogen for protein isolation and stored at −80 °C. Tissue was transferred in hypotonic buffer consisting of 10 mM HEPES (pH 7.9), 1.5 mM magnesium chloride, 10 mM potassium chloride, 10 mM 2-mercaptoethanol and protease inhibitor cocktail (Complete, Mini, EDTA-free tablets, Sigma Aldrich, St. Lois, MO, USA, Germany) as well as 1 mM phenylmethylsulfonyl fluoride (PMSF; Serva, Germany) and homogenized three times for 15 s with tissue homogenizer (Biospec, Bartlesville, OK, USA). The samples were left on ice for 15 min before adding Nonidet P40 (Sigma Aldrich, St. Lois, MO, USA) to a final concentration of 0.5% and then centrifuged at 3000 rpm for 1 min at 4 °C. The resulting supernatants were centrifuged at 14,000 rpm for 30 s at 4 °C. Obtained supernatants with cytoplasmic proteins were used for further procedure (Huber et al., 2007).

Proteins were separated by 10% (OPN) and 13,5% (MT-I + II) sodium dodecyl sulfate polyacrylamide gel electrophoresis (SDS–PAGE), under reducing (OPN) and non-reducing (MT-I + II) conditions and then transferred onto a nitrocellulose membrane (BioRad, Hercules, CA, USA). Membranes were blocked with 5% BSA (Sigma, Aldrich, St. Lois, MO, USA) in tris-buffered saline with 0.05% Tween-20 (TBST) and incubated with goat anti-OPN IgG antibody (R&D systems, Minneapolis, MN, USA; 1:500) and mouse anti-MT-I + II IgG_1 antibody (clone E9; Dako Cytomation, Glostrup, Danmark; 1:200), followed by incubation with species specific HRP-conjugated secondary antibodies. The rabbit anti-β-tubulin (Abcam, Cambridge, UK, 1:25,000) was used as a control of cytoplasmic proteins. The mouse anti-β-actin (Millipore, Darmstadt, Germany, 1:80,000) was used as a control of protein loading. For detection membranes were, incubated with Amersham ECL Prime (GE Healthcare, Sweden), and scanned with Kodak Image Station 440CF (Kodak, USA). The intensity of the bands was quantified using ImageJ software (http://rsb.info.nih.gov/ij/). To determine the relative expression of analyzed proteins in spinal cord of immunized animals and animals treated only with CFA, the band density of each sample was compared with the band intensity obtained from spinal cord of untreated animals after normalization to an internal control β-actin.

RNA extraction, reverse transcription and real-time PCR analysis

Spinal cords were collected from rats treated with BBH + CFA ($N = 4$), with CFA ($N = 4$) and from untreated ($N = 4$) rats. Samples were snap-frozen in liquid nitrogen for RNA isolation and stored at −80 °C. Total RNA was extracted from frozen tissues, using Trizol Reagent (Invitrogen, Carlsbad, CA, USA), according to the protocol provided by the manufacturer (1 ml of Trizol per 100 mg of tissue). RNA was assayed by ultraviolet spectrophotometric measurements at a wavelength of 260 nm, and its purity was estimated by the ratio of A260/A280. Total RNA (5 μg) was treated with turbo DNA-free reagent (Ambion; Applied Biosystems, Carlsbad, CA, USA) to remove possible contamination with genomic DNA, followed by reverse transcription (High Capacity cDNA Reverse Transcription Kit; Applied Biosystems, Carlsbad, CA, USA), according to the manufacturer's instructions. Relative expression levels of OPN and MT-1 mRNA were determined by real-time PCR analysis using SYBR Green PCR Universal Mastermix (Applied Biosystems, Carlsbad, CA, USA) according to the manufacturer's instructions. Oligonucleotide primers for rat OPN (forward 5′-ACAG TATCCCGATGCCACAG-3′; reverse 5′-GACT CATGGCTGGTCTTCCC-3′), rat MT-1 (forward 5′-CAC CGTTGCTCCAGATTCAC-3′; reverse 5′-GCAGCAG CACTGTTCGTCAC-3′) previously published (Banni et al., 2010) and rat β-actin (forward 5′-CCAC CAGTTCGCCATGGAT-3′; reverse 5′-CCATACCCAC CATCACACCC-3′) were obtained from Metabion (Planegg, Germany). ABI Prism 7300 Sequence Detector System (Applied Biosystems, Carlsbad, CA, USA) was used to perform quantitative PCR. Relative mRNA levels were determined after normalization to β-actin.

Statistical analysis

The statistical analyses were performed using Statistica software version 12 (StatSoft Inc., Tulsa, OK, USA). The distribution of data was tested for normality using the Kolmogorov–Smirnov test. Differences between groups were assessed with either one-way analysis of variance (ANOVA) followed by the post hoc Scheffé test or by Kruskal–Wallis and Mann–Whitney U test. Statistical differences with $p < 0.05$ were considered significant.

RESULTS

EAE was induced in genetically susceptible DA rats, which react on immunization with BBH in CFA by development of chronic-relapsing form of disease. It is characterized by appearance of two peaks of clinical symptoms, but since previously we found that MT-I transcription and MT-I + II immunoreactivity in neural tissues were significantly upregulated particularly during the first attack of EAE that occurs on day 13 or 14 after the immunization with BBH + CFA (Jakovac et al., 2011; Grubic-Kezele et al., 2013), in this study we sacrificed the rats, exhibiting stage 3 of disease (hind legs paralysis with incontinence) at the same time (Fig. 1). Expression profiles of OPN and MT-I + II were examined in spinal cord and in the brain and the data were compared with findings in untreated rats and in CFA-treated rats, sacrificed at the same post-immunization (p. i.) day. As shown on Fig. 1, these control rats, in contrast

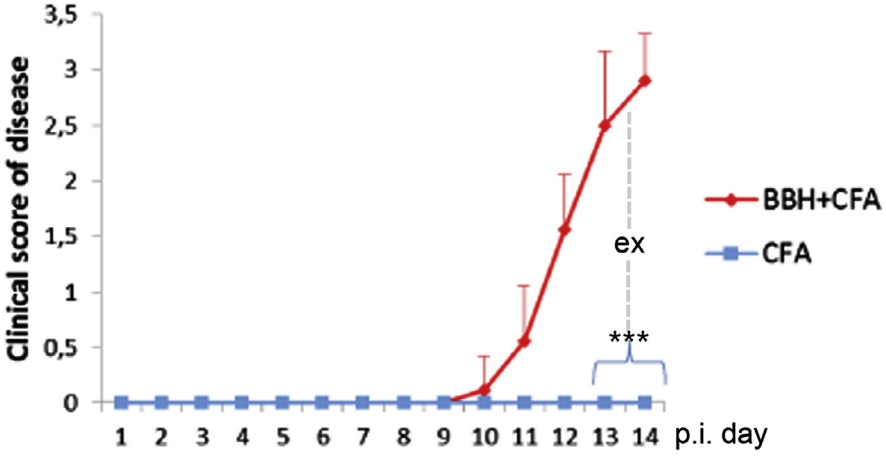

Fig. 1. Study design and clinical course of EAE in Dark Agouti (DA). Rats were immunized by injection of bovine brain homogenate (BBH) in complete Freund's adjuvant (CFA) or with CFA and examined daily for clinical signs of EAE and scored as: 0 – no symptoms; 1 – flaccid paralysis of tail; 2 – hind legs paresis; 3 – hind legs paralysis with incontinence and 4 – death of the animal. Pairs of BBH + CFA and CFA-treated rats were sacrificed on the 13th or on the 14th post-immunization (p.i.) day, i.e. at the time when rats immunized with encephalitogen exhibited hind legs paralysis with incontinence (stage 3 of disease). Data are mean ± SE (N = 10/group). $^{***}p < 0.001$). (Mann–Whitney U test).

to the animals treated with BBH + CFA, did not develop any clinical symptom of disease ($p < 0.001$).

Expression of OPN during the first relapse of EAE in spinal cord

Profiling of OPN mRNA and proteins by qPCR and Western blot (WB) showed that transcription of OPN gene was significantly greater in rats immunized with encephalitogen than in control rats (Fig. 2A; $p < 0.05$). Moreover, WB revealed that in these rats the cytoplasmic SC lysates contained more OPN fragments of small molecular length (32 kDa) than intact and CFA-treated rats (Fig. 2B, C; $p < 0.05$), implying that immunization had stimulated the proteolytic cleavage of OPN. Immunohistochemical data (Fig. 2D) also showed that OPN expression in EAE rats was highly upregulated around plaques (a) and on cells surrounding blood vessels in white matter (b, e, red head arrow), in choroid plexus and subarachnoid places (c, d), as well as in numerous motor neurons in the gray matter of spinal cord (f). The absence of these changes in rats treated with CFA (Fig. 2D g, h) confirmed that they were specific for encephalitogen. Besides, all slides used as negative controls, did not show any immunopositivity (Fig. 2D, inserts on g, h).

Expression of MT I + II during the first relapse of EAE in spinal cord

Simultaneously, in agreement with our previous results (Jakovac et al., 2011; Grubic-Kezele et al., 2013) we found that immunization markedly elevated also the transcription of MT-I gene (Fig. 3A) and augmented the content of MT I + II proteins in lysates of spinal cord (Fig. 3B, C). ($p < 0.001$ in comparison with intact and CFA-treated rats). As shown in Fig. 3 D, MTs were upregulated diffusely in parenchyma of SC (a–f), in subependymal zones around the central canal (a, b, e), on several astrocytes (d, insert), as well as on blood vessels endothelial cells (f, head arrows). Furthermore, a very high MT immunoreactivity was found in neurons (c, f), suggesting that they were similar to those expressing OPN (Fig. 2D f). In contrast, the expression of MT-I + II in spinal cord of CFA-treated rats was absent or very low (Fig. 3D g, h). Beside, in negative controls the immunopositivity was not observed (Fig. 3D inserts on g, h).

Relationship of OPN to CD3, GFAP, CD44 and αVβ3 in the spinal cord

By double immunofluorescent analyses we next tried to determine the type of cells that express OPN and the relationship of OPN to its receptors CD44 and αVβ3 integrin. The data have shown (Fig. 4 A) that within the spinal cord of EAE rats were present several CD3+ lymphocytes (a) and GFAP+ astrocytes (d). They, however, did not co-express OPN (c, f), implying that during the first attack of EAE, OPN was more expressed on other types of mononuclear cells. In the affected tissue were also present cells expressing CD44 (g), but they also did not co-express OPN (i). In contrast, a high OPN-immunoreactivity was found in almost all neurons expressing αVβ3 integrin (l, arrows). Moreover, as emphasized on Fig. 4B (a–c, arrows), many of them contained OPN-positive granular deposits in perinuclear location, suggesting that, in these neurons OPN was directed to secretory pathway. Double staining for OPN and GM 130, a marker of Golgy, confirmed this hypothesis (Fig. 4B e–g, arrows), and labeling of OPN and NeuN confirmed that the accumulation of OPN-positive granular deposits occurred in mature neurons (Fig. 4B h–j). Noteworthy, similar findings were not found in CFA-treated rats (Fig. 4B d), showing that upregulation of OPN in αVβ3+ neurons was specific for the encephalitogen-induced processes. On slides used as negative controls fluorescent signals were not detected at all (not shown).

Co-expression of OPN and MT-I + II in the spinal cord

Immunofluorescent analyses confirmed that during the attack of EAE in spinal cord arose the expression of MT-I + II (Fig. 5A) on blood vessels endothelial cells (a, arrow), on agglomerates of mononuclear cells (d), as well as on neurons (g) and some stromal αVβ3+ cells (j). OPN-positive cells around the vessels (b) did not express MT (c, arrow), but MT+ cells in agglomerates (d) expressed also a high OPN immunoreactivity (f). Moreover, the co-staining of MTs and OPN was found in soma of numerous neurons (i). In these MT+ neurons, OPN was visible in granular deposits

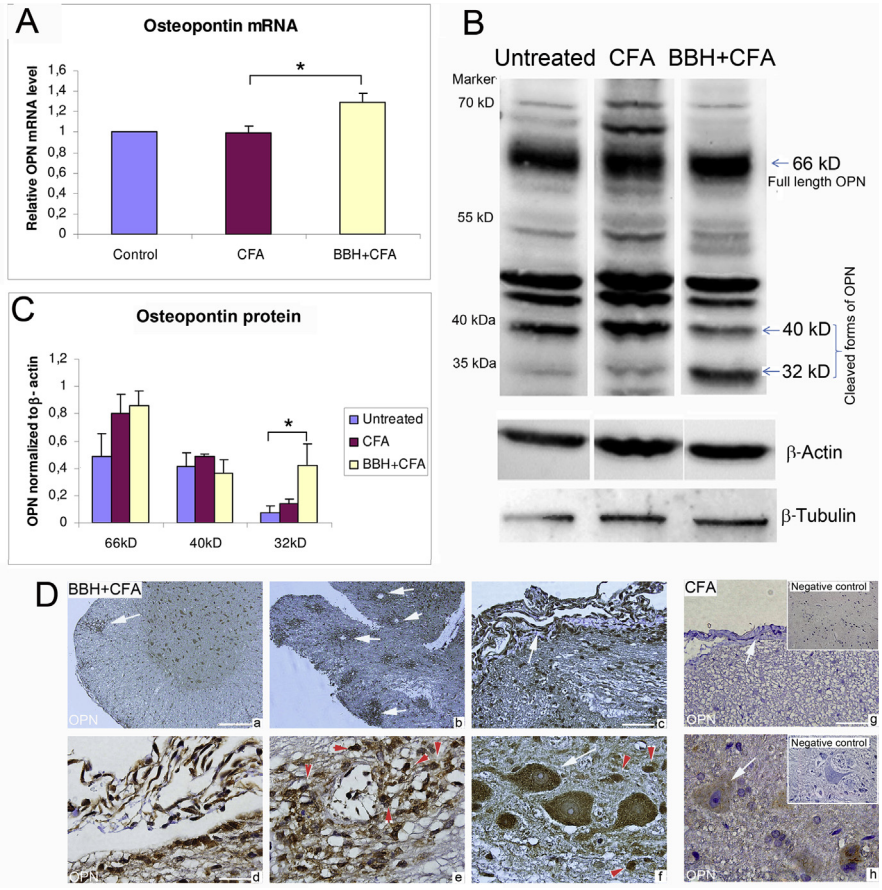

Fig. 2. OPN transcription, proteolytic cleavage and protein expression are increased in spinal cord (SC) during the first relapse of EAE. Samples of lumbar SC were obtained from untreated rats, from rats treated by CFA and from rats exhibiting hind led paralysis after treatment with brain homogenate (BBH) in complete Freund's adjuvant (CFA)(post-immunization day 13 or 14). (A) Relative expression levels of OPN mRNA (normalized to β-actin), determined by real-time PCR ($N = 4$). (B) Representative, original Western blots of cytoplasmic fraction of SC, showing different OPN forms (full length OPN – 66 kDa and cleaved forms of OPN – 40 kDa and 32 kDa), β-actin (used as a loading control) and β-tubulin (used as cytoplasmic marker) ($N = 3$). (C) Expression of OPN protein in cytoplasmic fraction shown as OPN/β-actin ratio. Values refer to means ± SEM. (D) Immunohistochemical staining of OPN protein in paraffin-embedded sections of the lumbar SC tissue in DA rats treated by BBH + CFA (a–f) or CFA (g, h). Arrows on (a–c) point to areas of plaque, blood vessels and choroid plexus, respectively. Red arrow heads on (e) point to upregulation of OPN on lymphoid cells around the blood vessels. Inserts on (g) and (h) show tissue staining in section incubated without primary anti-OPN antibodies (negative control). The results are representative findings of three rats. $^{*}p < 0.05$ (One-way ANOVA followed by the post hoc Scheffé test or Kruskal–Wallis test). Scale bars 100 μm (a, b), 20 μm (c, g) and 10 μm (d–f, h). (For interpretation of the references to color in this figure legend, the reader is referred to the web version of this article.)

(Fig. 5B b, arrow), but also as homogenous, cytoplasmic and nuclear immunostaining (Fig. 5A i and B a, c, head arrows), suggesting that OPN might be located also outside of the secretory vesicles. Similar changes were not observed in CFA-treated rats (Fig. 5B d).

Expression and tissue distribution of OPN in the brain

The data obtained by immunohistochemistry clearly showed that during first relapse of EAE the OPN expression was markedly upregulated (Fig 6a–l) in comparison with findings in CFA-treated rats (Fig. 6m–p) in following locations: choroid plexus (a), in subependymal area (b, c), in group of large cells in subventricular zone (d), in cortex (e), in oligodendrocyte-like cells in white matter (f), in hippocampus (CA1, gyrus dentatus and subgranular zone; g–i, respectively), as well as in cerebellum (Purkinje cells and medullar neurons; j–l).

Relationship of OPN to cells expressing αVβ3 in the brain

Owing to the findings in SC (Fig. 4), in the brain of rats treated by BBH + CFA we estimated particularly the relationship of OPN to neurons expressing $\alpha V\beta 3$. The data (Fig. 7) clearly showed that OPN-immunoreactivity was present in cortical $\alpha V\beta 3+$ neurons (a–c) and in several large cells located in subventricular zone (d–f). Co-staining of OPN and $\alpha V\beta 3$ was found also on Purkinje cells in cerebellum (j–l). $\alpha V\beta 3$ was highly upregulated also in granular cell layer (GCL) of hippocampus, but only some of these neurons expressed OPN immunoreactivity (g–i). However, as emphasized in Fig. 7B, almost all $\alpha V\beta 3+$ cortical cells (a–c, arrows) and NeuN + neurons (h–j) exhibited high granular OPN immunoreactivities in structures stained with GM 130 antibodies (e-g, arrows), confirming that in these neurons OPN was confined to the secretory pathways. In control, CFA-treated rats, moderate expression of integrin $\alpha V\beta 3$ was noticed in the hippocampus (not shown), but in contrast to findings in BBH + CFA treated rats, cortical neurons of control rats did not co-express OPN (Fig. 7 B d *versus* F A c).

Relationship of OPN to MT-I + II in the brain

Single and double labeling of brain sections for OPN and MT in EAE rats showed that OPN and MT-I + II were co-expressed in numerous cortical neurons (Fig. 8A a–c; B a), in Purkinje cells in cerebellum (A j–l) and some cells located n GCL of hippocampus (A g–i, arrows). In corresponding brain areas of rats treated only with CFA the similar changes were not found (Fig. 8A, inserts on c, f, i, l). A high, encephalitogen-induced, co-staining of MTs and OPN was found also in the choroid plexus (Fig. 8B c *versus* d), as well as on large cells in subventricular zone (SVZ) (Fig. 8A d–f; B b, arrows), which has been considered responsible for the expansion and proliferation of the stem/progenitors

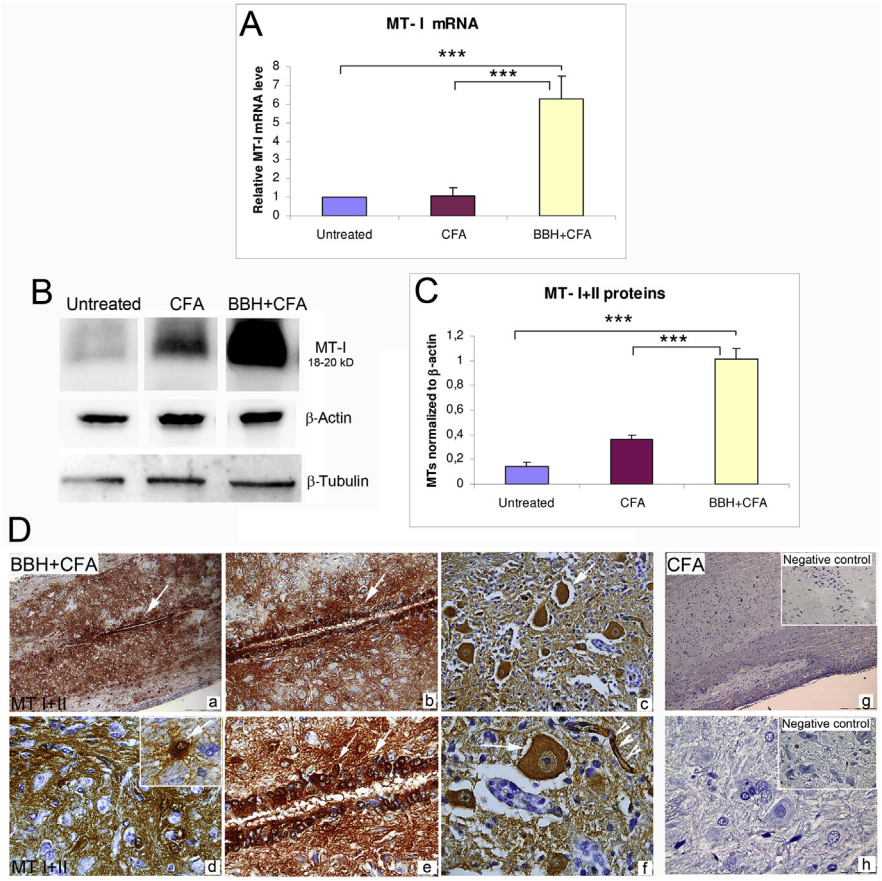

Fig. 3. Metallothionein (MTs) transcription and protein expression are increased in spinal cord (SC) during the first relapse of EAE. Samples of lumbar SC were obtained from untreated rats, from rats treated by CFA and from rats exhibiting hind led paralysis after treatment with brain homogenate (BBH) in complete Freund's adjuvant (CFA) (post-immunization day 13 or 14). (A) Relative expression levels of MT-I mRNA (normalized to β-actin), determined by real-time PCR ($N = 4$). Values refer to mean ± SEM. (B) Representative original Western blots of cytoplasmic fraction of SC showing MT-I + II, β-actin (used as a loading control) and β-tubulin (used as cytoplasmic marker) ($N = 3$). (C) Expression of MT I + II proteins in cytoplasmic fraction shown as MTs/β-actin ratio. (D) Immunohistochemical staining of MT I + II protein in paraffin-embedded sections of the lumbar SC tissue in DA rats treated by BBH + CFA (a–f) or CFA (g–h). Arrows on (a, b, e) point to central canal. Insert on (d) show astrocyte. Head arrows on (f) point to blood vessel. Inserts on (g) and (h) show tissue staining in section incubated with isotypic IgG (negative control). The results are representative findings of three rats. $^{*}p < 0.05$ (One way ANOVA followed by the post hoc Scheffé test or Kruskal–Wallis test). Scale bars 100 μm (a, g), 20 μm (b, c) or 10 μm (d–f, h).

during brain repair (Alvarez-Buylla et al., 2001; Alagappan et al., 2009). Our data, showing the presence of PCNA in these cells (Fig. 8A e, inserted picture) seem to support this possibility and imply that OPN and MT-I + II might influence their proliferation. Interestingly, in these MT+/PCNA+ cells OPN immunoreactivity was not found in perinuclear granules, but in patches adjacent to the plasma membrane (Fig. 8A f, B b), suggesting that in these mitotically active neuronal progenitors OPN was present outside of the secretory pathway.

DISCUSSION

Profound influences of OPN and ECM on basic cellular processes that affect the pathogenesis of MS and EAE have been repeatedly suggested (Steinman, 2009; Niino and Kikuchi, 2011; Brown, 2012; Plantman, 2013; Kahles et al., 2014; Rittling and Singh, 2015; Subraman et al., 2015). However, although it is known that OPN is one of the genes most highly expressed in autoimmune demyelinating lesions (Chabas et al., 2001), as well as that it contributes to the development of cell-mediated inflammatory responses (O'Regan et al., 2000; Cantor and Shinohara, 2009; Inoue and Shinohara, 2011; Rittling and Singh, 2015), the complex interplay between supportive and inhibitory molecules in these events is not yet fully understood, similarly as the mechanisms that lead to the generation of functionally distinct forms of OPN during an autoimmune attack.

The data presented in this report are generally in line with the updated knowledge about the expression of OPN in EAE (Niino and Kikuchi, 2011), but the results point also to the relatively unknown interactions of OPN with MT I + II, implying that in some cells the pro-inflammatory properties of OPN can be balanced by the activation of cytoprotective, MT-related pathways, or that MT may enhance the pro-regenerative and anti-apoptotic properties of OPN. Hypothesis is based on our findings that during peak stage of EAE mRNA and protein expression of OPN arose concurrently with the transcription of MT-I and expression of MT-I + II proteins (Figs. 2 and 3) and that several inflammatory cells, glial cells and neurons in the spinal cord and in the brain express both OPN and MT I + II immunoreactivities (Figs. 4–5, 7–8). The data also suggest that these interactions might be linked with the proteolytic cleavage and posttranslational modification of OPN, since we found that cytoplasmic fraction of SC lysates from EAE rats contained greater amount of OPN with low molecular weight (32 kDa) than corresponding fractions obtained from CFA-treated and intact rats (Fig. 2B, C). This hypothesis seems to be supported by findings that OPN fragments of 40, 32, and 25 kDa may be generated by cleavage of OPN with MMP-3 (stromelysin-1) and MMP-7 (matrilysin) (Agnihotri et al., 2001; Gao et al., 2004) and by data showing that the N- and C-terminal fragments of OPN (with approx 35 kDa and 25 kDa, respectively) may be produced by cleavage of OPN by thrombin (Morimoto et al., 2010; Boggio et al., 2016). In our study the proteolytic cleavage of OPN should be better defined by the use of mAb specific for OPN sequences and by determination of functional activity of the generated segments, but it is noteworthy

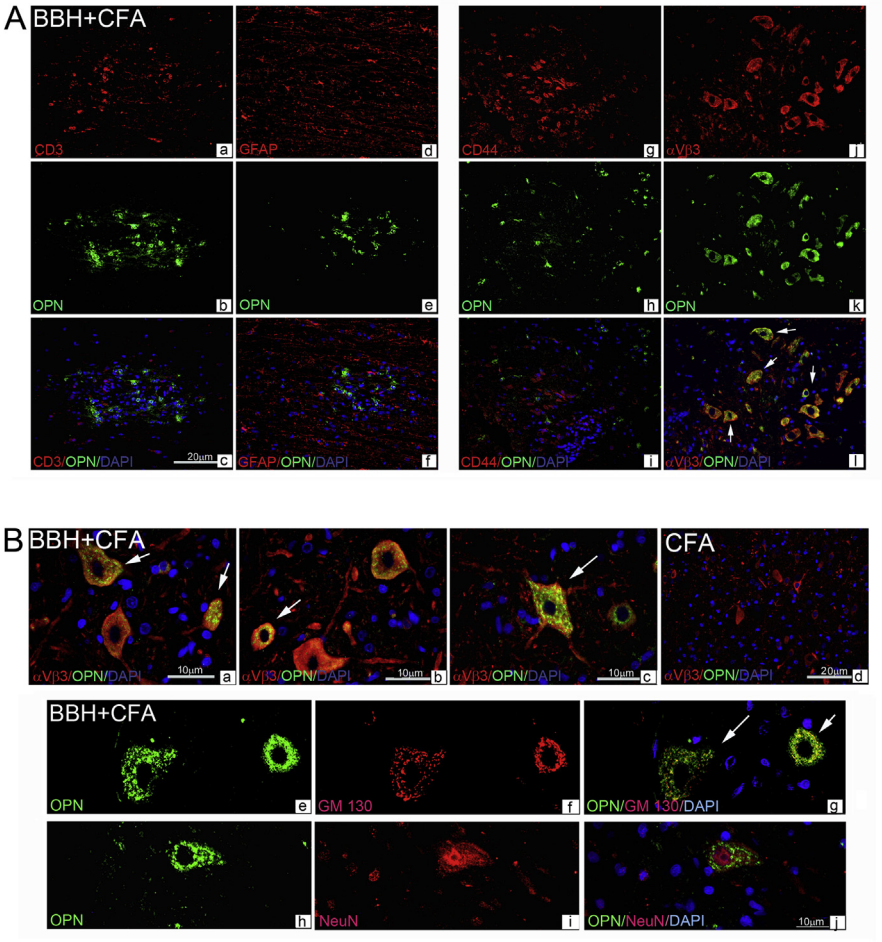

Fig. 4. Relationship of OPN to T lymphocytes, astrocytes and cells expressing CD44 and αVβ3 integrin. (A) T lymphocytes (a), astrocytes (d) CD44 (g) and αVβ3 (j) expressing cells were detected by anti-CD3, anti-GFAP, anti-CD44 and anti-αVβ3, respectively (red staining) in paraffin sections of SC tissue removed on the 13th–14th post-immunization day from paralyzed EAE rats (a–l). Green marks OPN staining by anti-OPN antibodies, blue marks DAPI staining of nuclei and yellow marks the overlapping of OPN with other markers. (B) Representative images ($N = 3$) show granular OPN deposits in αVβ3+ (a–c, arrows) and NeuN+ (h–j) neurons of EAE rats, as well as their accumulation in secretory vesicles of Golgy, labeled by anti-GM 130 monoclonal antibodies (e–g, arrows). Scale bars: 20 μm (A a–l, B d); 10 μm (B, a–c, e–j). (For interpretation of the references to color in this figure legend, the reader is referred to the web version of this article.)

that OPN fragments generated by proteolysis may exhibit new properties and expose higher adhesive activities for integrins, owing to the exposure of RGD motif and a cryptic SVVYGLR or SLAYGLR segments on N-terminal fragment of OPN molecule (Agnihotri et al., 2001; Gao et al., 2004; Boggio et al., 2016). In this context Boggio and co-workers (2016) recently clearly showed the recombinant proteins corresponding to the full length OPN and thrombin-cleaved OPN forms (OPN-N and OPN-C), exerted different effects on adhesive, migratory and secretory activity of T cells and monocytes and other crucial processes that contribute to the homing of autoreactive lymphocytes and formation of demyelinating lesions in the CNS. Moreover, underlining that thrombin-mediated cleavage of OPN plays a key role also *in vivo* these authors showed that administration of OPN-FL, OPN-C and OPN-C + OPN-N in the remission phase of disease induced a prompt relapse of EAE in mice immunized with MOG35–55, as well as that OPN-FL was much more effective in inducing EAE relapses than OPN-FL_{mut}, which was resistant to thrombin-mediated cleavage (Boggio et al., 2016). Similarly, Goncalves DaSilva and co-workers (2010) demonstrated that OPN mRNA and protein expression in the spinal cord of EAE-afflicted mice arose concurrently with MMP-12 expression, as well as that OPN-immunoreactive bands in the spinal cord of EAE mice had a pattern similar to MMP-12 cleavage of recombinant OPN *in vitro*. Interestingly, their data also showed that cleavage of OPN by MMP-12 might be beneficial for EAE mice, since in MMP-12$^{-/-}$ mice the exacerbated EAE was found (Goncalves DaSilva et al., 2010).

Furthermore, for our data it may be relevant that Morisaki et al. (2016) in rodent models of amyotrophic lateral sclerosis (ALS), found that OPN in spinal motor neurons stimulated MMP-9 transcription and expression through αvβ3 integrin-mediated transduction. In this condition the activation of OPN-integrin αvβ3-MMP-9 axis has been viewed as a sign of selective motor neurons vulnerability and second-wave neurodegeneration in ALS, but the contribution of these processes to active remodeling of neurons was also emphasized (Morisaki et al., 2016).

Our data, showing that in SC of EAE-rats are generated OPN fragments of small size (Fig. 1B, C), as well as that in numerous αVβ3+ neurons (Figs. 5 and 8) are present both OPN and MT proteins (Figs. 5 and 8), imply that in coordinated molecular response activated after intraneuronal distress participate not only OPN and MMP, but also the metal binding proteins – MT-I + II. The underlining mechanisms of this cross talk are unclear, but taken into account the evidence pointing to detrimental functions of OPN in EAE (Chabas et al., 2001; Jansson et al., 2002; Kim et al., 2004; Brown, 2012) and those showing that MT-I + II have marked cytoprotective, anti-inflammatory and neuroprotective properties (Hidalgo et al., 1991; Mocchegiani et al., 2000; Penkowa et al., 2003; Penkowa and Hidalgo, 2003; Penkowa, 2006; Pedersen et al., 2009; Manso et al., 2011) we may speculate that molecular changes induced by MTs in cellular compartment might restrain the pro-inflammatory effects of OPN or increase the anti-inflammatory properties of OPN and viability of target cells. Effects might be related with the ability of MT to serve as a storage protein from

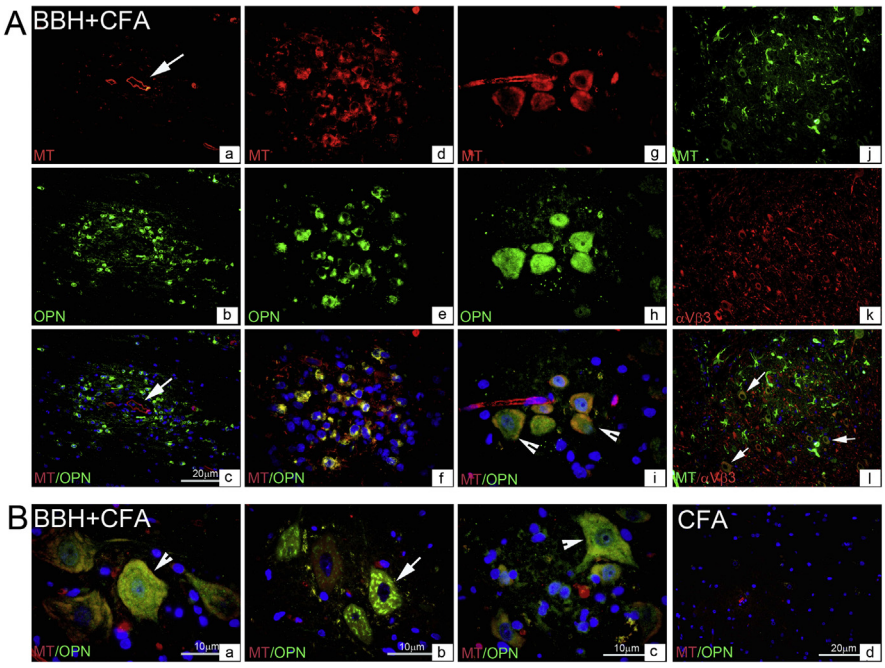

Fig. 5. Expression of MT-I + II and OPN in spinal cord during first relapse of EAE. (A) Cells expressing MTs, OPN and αVβ3 were detected with anti-MT-I + II (a, d, g – red staining; j – green staining), with anti-OPN (b, e, h – green staining), and with anti-αVβ3 antibodies (k – red staining) respectively, in paraffin sections of tissue obtained from rats treated with BBH + CFA (a–l). Blue marks DAPI staining of nuclei and yellow marks the overlapping of OPN with other markers. (B) Representative images ($N = 3$) show granular OPN deposits (b, arrow), cytoplasmic and nuclear OPN immunoreactivities (a, c, arrow heads) in EAE rats and findings in CFA-treated rats (d). Scale bars: 20 μm (A a–l, B d); 10 μm (B a–c). (For interpretation of the references to color in this figure legend, the reader is referred to the web version of this article.)

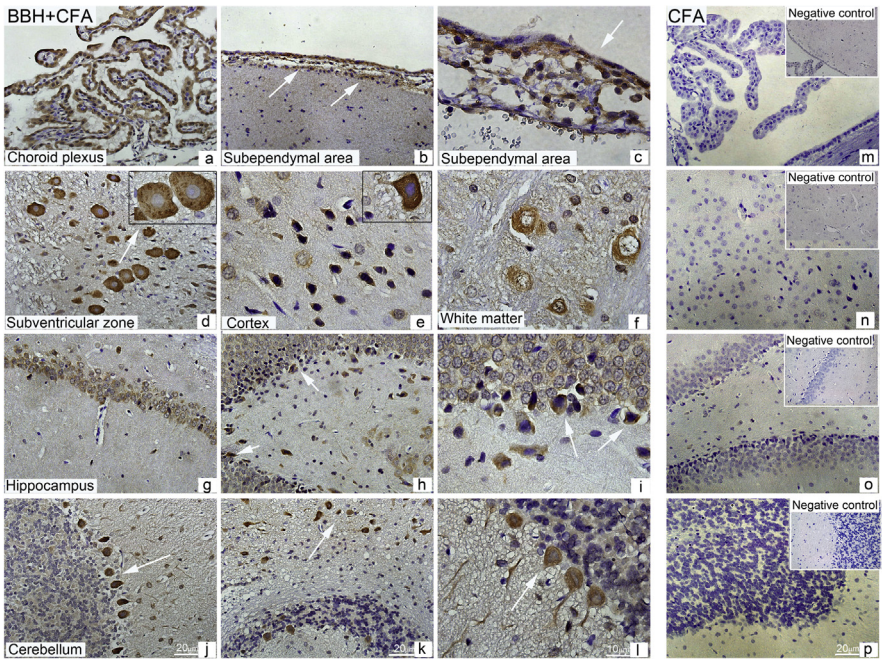

Fig. 6. Expression of OPN in brain regions during first relapse of EAE. Brain tissue was obtained from rats treated with BBH + CFA (a–l) or from CFA-treated rats (m–p). Paraffin sections were immunostained for OPN and counterstained with hematoxylin. Inserts on (m–p) show tissue staining in section incubated without primary anti-OPN antibodies (negative control). The results are representative findings of three rats. Scale bars: 20 μm or 10 μm (third column and inserts on m–o).

which labile zinc can be mobilized by cysteine oxidation, as well as with its ability to act as antagonist of toxic metals and organic molecules, as scavenger of reactive oxygen and nitrogen species and as a regulator of zinc-finger and p53 and other metal-containing transcription factors (Andrews, 2000; Davis and Cousins, 2000; Mocchegiani et al., 2000; Lynes et al., 2006; Rink and Haase, 2007; Inoue et al., 2009; Isani and Carpene, 2014; Ling et al., 2016). Moreover, for our data showing OPN/MT co-expression in neurons (Figs. 5 and 8) it may be particularly relevant that MTs may prevent demyelination and axonal damage and increase oligodendrocyte precursors proliferation during EAE (Penkowa and Hidalgo, 2003) and preserve the mitochondrial structural and functional integrity by augmentation of mitochondrial coenzyme Q10, glutathione, ferritin, melatonin, and neuromelanin synthesis in neurons (Sharma et al., 2013).

As shown by Ambjřrn and coworkers (2008), the survival-promoting effects of MT and its synthetic analog EmtinB on neurons include binding of MT to surface receptors of the low-density lipoprotein receptor (LDLR) family, such as megalin and lipoprotein receptor-related protein-1, and activation of signal transduction pathways that promote neurite outgrowth and survival or abrogate the apoptosis. In this context we may speculate that binding of MT to multiligand, surface receptors might affect also the OPN-αvβ3 integrin-MMP-9 axis and other post-translational processes, such as phosphorylation, glycosylation and sulfation that determine OPN signaling and its functions in various cell types (Kazanecki et al., 2007; Kahles et al., 2014)..This speculation, however, remains to be proved, similarly as the possibility that MT/zinc network affects the cell-autonomous immune mechanisms in neurons that trigger a pathogenic cascade after binding of endogenous molecules produced by stress (heat shock proteins, mRNA, fibrinogen, mitochondrial DNA) to TLRs in injured cells (Czirr and Wyss-Coray, 2012). Noteworthy, TLR3, -7, -8, and -9 are located in the ER and endosomal

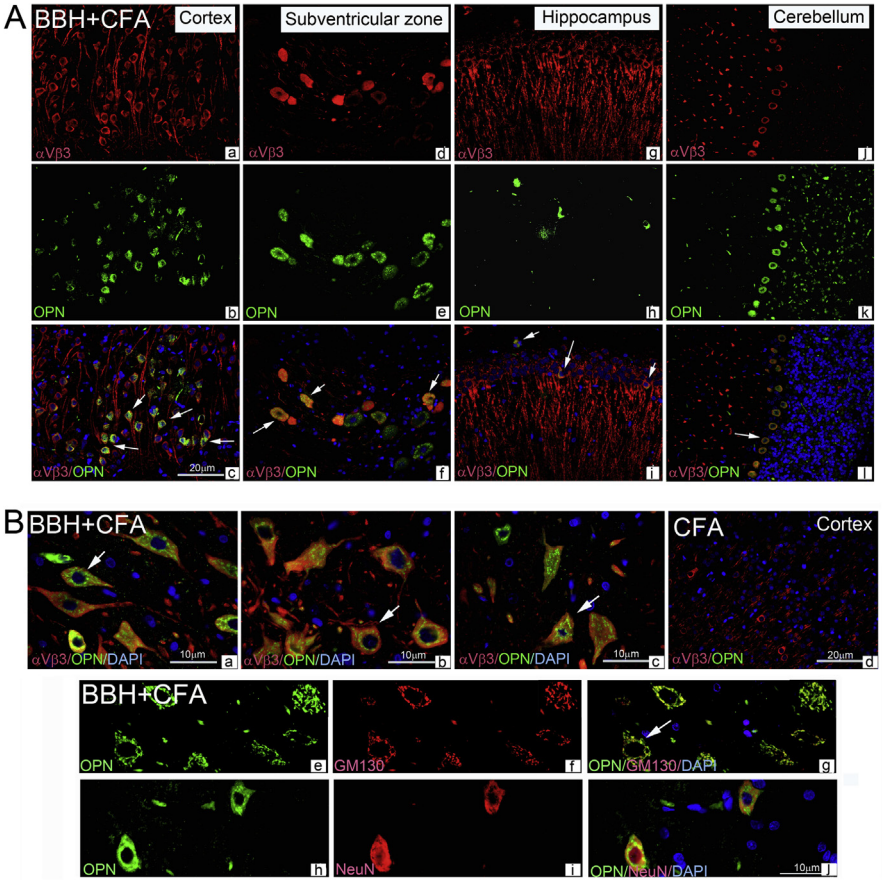

Fig. 7. Relationship of OPN to cells expressing αVβ3 in the brain during first relapse of EAE. (A) Cells expressing αVβ3 integrin and OPN were detected with anti-αVβ3 (red staining) and anti-OPN (green staining) antibodies, respectively, in paraffin sections of tissue obtained from rats treated with BBH + CFA (a–l). Blue marks DAPI staining of nuclei and yellow marks the overlapping of OPN with αVβ3. (B) Representative images ($N = 3$) show granular OPN deposits in cortical αVβ3 + (a–c) and NeuN+ (h–j) neurons, as well as their accumulation in secretory vesicles of Golgy, labeled by anti-GM 130 monoclonal antibodies (e–g) in EAE rats and findings in CFA-treated rats (d). Scale bars: 20 μm (A a–l, B d); 10 μm (B a–c, e–j). (For interpretation of the references to color in this figure legend, the reader is referred to the web version of this article.)

compartments, where we found OPN-positive granular deposits (Figs. 4, 7), and their activation can lead to initiation of autophagy and induce the clearance of defective organelles or protein aggregates (Czirr and Wyss-Coray, 2012). Moreover, it should be taken into account that the cytosolic Zn level is regulated also by Zn transporters of the Slc39/ZIP and Slc30/ZnT families and that Zn may function as an intracellular signaling molecule or second messenger, either independently, or in a manner dependent on the transcriptional changes of Zn transporters or MTs (Fukada et al., 2011).

Altogether, these evidence imply that the outcome of OPN/MT interaction in neurons might be the abrogation of detrimental functions of OPN or the stimulation of pro-regenerative and anti-apoptotic properties of OPN (Carecchio and Comi, 2011; Plantman, 2013) The latter, is emphasized also by findings that recombinant OPN upregulates myelination and remyelination in *in vitro* cellular cultures (Selvaraju et al., 2004), by data showing that RGD-containing peptide fragment of OPN protects dopaminergic neurons against toxic insult (Iczkiewicz et al., 2010), as well as by findings that OPN stimulates neurite growth of hippocampal neurons (Plantman, 2012) and facilitates the regeneration of motor neuron axons (Wright et al., 2014).

Herein we also show that during first attack of EAE the expression of OPN and MT-I + II increases at sites of cellular invasion and T cell reactivation, such as BBB, choroid plexus and leptomeninges around the spinal cord (Figs. 3, 4), as well as that several ependymal cells and inflammatory cells around the blood vessels in demyelinating plaques co-localize OPN and MT (Fig. 8). These data are in high agreement with evidence showing that both OPN (Shinohara et al., 2008a; Cantor and Shinohara, 2009; Morimoto et al., 2010; Inoue and Shinohara, 2011; Hellewell and Adams, 2015) and MT/Zn network have high impact on innate and adaptive immunity (Mocchegiani et al., 2000; Prasad, 2008; Fukada et al., 2011; Haase and Rink, 2014). The mechanisms of OPN/MT interaction in our experimental model, however, remain to be elucidated, since in the development of EAE are involved various cell types and different OPN isoforms (Cantor and Shinohara, 2009). Thus, the plasmacytoid DC, containing i-OPN, may be more responsible for the generation of pro-inflammatory TH17 cells and the onset of EAE (Shinohara et al., 2008a). In contrast, it is likely that s-OPN, produced by activated T-cells, contributes more to the development of relapse and progression of EAE (Hur et al., 2007). However, as shown by Boggio et al. (2016) the OPN activity in all these steps may be dependent on thrombin-induced cleavage, since OPN effects on IL-17 and IL-6 secretion and cell migration were mainly ascribable to OPN-N, whereas those on IL-10 secretion and cell adhesion were mainly mediated by OPN-C.

Our data imply that during first attack of EAE OPN and MTs were more expressed in monocyte and microglia-like cells (Fig. 5A f) and that OPN activities were more related to its RGD-binding domain of OPN than to OPN-C fragment, but in spite of the fact that these findings are in line with current knowledge showing that binding of RGD fragment of many ECM proteins leads to activation and conformational change of integrin receptor and activation of an "outside-in" and an "inside-out" signaling cascades (Wu and Reddy, 2012) our study requires additional phenotypic and functional analyses.

In conclusion our data show that acute phase of EAE in DA rats is followed by increased transcription of OPN

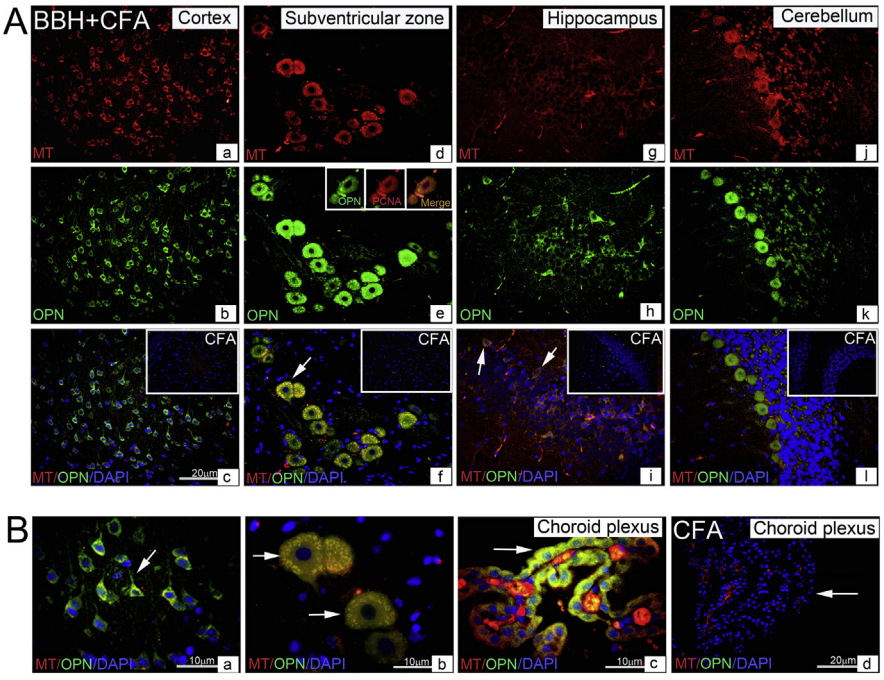

Fig. 8. Expression of MT-I + II and OPN in the brain during first relapse of EAE. (A) Cells expressing MTs and OPN were detected by the use of anti MT-I + II (red staining) and anti-OPN antibodies (green staining), respectively in paraffin sections of tissue obtained from rats treated with BBH + CFA (A a–l) and rats treated only with CFA (inserts on A c, f, i, l). Embedded picture on (e) shows the presence of proliferating cellular nuclear antigen (PCNA) (red staining). Blue marks DAPI staining of nuclei and yellow marks the overlapping of OPN with MT-I + II or PCNA. B) Representative images ($N = 3$) show OPN immunoreactivity in cortical neurons (a), in subventricular zone (b) and in choroid plexus (c) of EAE rats and findings in choroid plexus of CFA-treated rats (d). Scale bars: 20 μm (A a–l, B d); 10 μm (B a–c). (For interpretation of the references to color in this figure legend, the reader is referred to the web version of this article.)

and MT-I gene, by signs of proteolytic cleavage of OPN and increased synthesis of MT-I + II proteins in SC, by enhanced expression of OPN and MT proteins in the spinal cord and in the brain, as well as by co-expression of OPN and MTs in numerous cells, implying that during autoimmune attack the harmful properties of OPN might be, particularly in αvβ3+ neurons, restrained by cytoprotective activities of MTs.

AUTHORS' CONTRIBUTION

HJ and TGK performed all *in vivo* experiments and immunohistochemistry, TGK and SS performed Western blotting and PCR analysis, BMJ designed the research study, BRS designed the research study and wrote the paper. All authors analyzed and reviewed the results and approved the final version of the manuscript.

COMPETING INTERESTS

The authors declare that they have no competing interests.

Acknowledgments—This work was supported by grants from the University of Rijeka, Croatia (projects 13.06.1.1.16 (BRS), 13.06.2.2.58 (HJ) and 13.06.1.1.08 (BMJ) and by grant supported by Croatian Science Foundation (HRZZ, project 3432; BMJ).

REFERENCES

Agnihotri R, Crawford H, Haro H, Matrisian L, Havrda M, Liaw L (2001) Osteopontin, a novel substrate for matrix metalloproteinase-3 (stromelysin-1) and matrix metalloproteinase-7 (matrilysin). J Biol Chem 276:28261–28267.

Alagappan D, Lazzarino DA, Felling RJ, Balan M, Kotenko SV, Levison SW (2009) Brain injury expands the numbers of neural stem cells and progenitors in the SVZ by enhancing their responsiveness to EGF. ASN NEURO 1:e00009.

Alvarez-Buylla A, Garcia-Verdugo JM, Tramontin AD (2001) A unified hypothesis on the lineage of neural stem cells. Nat Rev Neurosci 2:287–293.

Ambjørn M, Asmussen JW, Lindstam M, Gotfryd K, Jacobsen C, Kiselyov VV, Moestrup SK, Penkowa M, Bock E, Berezin V (2008) Metallothionein and a peptide modeled after metallothionein, EmtinB, induce neuronal differentiation and survival through binding to receptors of the low-density lipoprotein receptor family. J Neurochem 104:21–37.

Andrews GK (2000) Regulation of metallothionein gene expression by oxidative stress and metal ions. Biochem Pharmacol 59:95–104.

Ashkar S, Weber GF, Panoutsakopoulou V, Sanchirico ME, Jansson M, Zawaideh S, Rittling SR, Denhardt DT, Glimcher MJ, Cantor H (2000) Eta-1 (osteopontin): an early component of type-1 (cell-mediated) immunity. Science 287:860–864.

Banni M, Messaoudi I, Said L, El Heni J, Kerkeni A, Said K (2010) Metallothionein gene expression in liver of rats exposed to cadmium and supplemented with zinc and selenium. Arch Environ Contam Toxicol 59:513–519.

Bellachene A (2008) Small integrin-binding ligand N-linked glycoprotein's (SIBLINGs): multifunctional proteins in cancer. Nat Rev Cancer 8:212–226.

Boggio E, Dianzani C, Gigliotti CL, Soluri MF, Clemente N, Cappellano G, Toth E, Raineri D, Ferrara B, Comi C, Dianzani U, Chiocchetti A (2016) Thrombin cleavage of osteopontin modulates its activities in human cells in vitro and mouse experimental autoimmune encephalomyelitis in vivo. J Immunol Res 2016:1–13.

Braitch M, Constantinescu CS (2010) The role of osteopontin in experimental autoimmune encephalomyelitis (EAE) and multiple sclerosis (MS). Inflamm Allergy Drug Targets 9:249–256.

Brown A (2012) Osteopontin: a key link between immunity, inflammation and the central nervous system. Transl Neurosci 3:288–293.

Cantor H, Shinohara ML (2009) Regulation of T-helper-cell lineage development by osteopontin: the inside story. Nat Rev Immunol 9:137–141.

Carecchio M, Comi C (2011) The role of osteopontin in neurodegenerative diseases. J Alzheimers Dis 25:179–185.

Chabas D, Baranzini SE, Mitchell D, Bernard CC, Rittling SR, Denhardt DT, Sobel RA, Lock C, Karpuj M, Pedotti R, Heller R, Oksenberg JR, Steinman L (2001) The influence of the proinflammatory cytokine, osteopontin, on autoimmune demyelinating disease. Science 294:1731–1735.

Coyle P, Philcox JC, Carey LC, Rofe AM (2002) Metallothionein: the multipurpose protein. Cell Mol Life Sci 59:627–647.

Czirr E, Wyss-Coray T (2012) The immunology of neurodegeneration. J Clin Invest 122:1156–1163.

Davis SR, Cousins RJ (2000) Metallothionein expression in animals: a physiological perspective on function. J Nutr 130:1085–1088.
Denhardt DT, Noda M, O'Regan AW, Pavlin D, Berman JS (2001) Osteopontin as a means to cope with environmental insults: regulation of inflammation, tissue remodeling, and cell survival. J Clin Invest 107:1055–1061.
Fedarko NS, Jain A, Karadag A, Fisher LW (2004) Three small integrin binding ligand N-linked glycoproteins (SIBLINGs) bind and activate specific matrix metalloproteinases. FASEB J 18:734–736.
Fisher LW, Torchia DA, Fohr B, Young MF, Fedarko NS (2001) Flexible structures of SIBLING proteins, bone sialoprotein, and osteopontin. Biochem Biophys Res Commun 280:460–465.
Fukada T, Yamasaki S, Nishida K, Murakami M, Hirano T (2011) Zinc homeostasis and signaling in health and diseases. Zinc signaling. J Biol Inorg Chem 16:1123–1134.
Gao YA, Agnihotri R, Vary CPH, Liaw L (2004) Expression and characterization of recombinant osteopontin peptides representing matrix metalloproteinase proteolytic fragments. Matrix Biol 23:457–466.
Goncalves DaSilva A, Liaw L, Yong VW (2010) Cleavage of osteopontin by matrix metalloproteinase-12 modulates experimental autoimmune encephalomyelitis disease in C57BL/6 mice. Am J Pathol 177:1448–1458.
Green P, Ludbrook S, Miller D, Horgan C, Barry S (2001) Structural elements of the osteopontin SVVYGLR motif important for the interaction with alpha(4) integrins. FEBS Lett 503:75–79.
Grubic-Kezele T, Jakovac H, Tota M, Canadi-Juresic G, Barac-Latas V, Milin C, Radosevic-Stasic B (2013) Metallothioneins I/II expression in rat strains with genetically different susceptibility to experimental autoimmune encephalomyelitis. Neuroimmunomodulation 20:152–163.
Guan H, Nagarkatti PS, Nagarkatti M (2011) CD44 Reciprocally regulates the differentiation of encephalitogenic Th1/Th17 and Th2/regulatory T cells through epigenetic modulation involving DNA methylation of cytokine gene promoters, thereby controlling the development of experimental autoimmune encephalomyelitis. J Immunol 186:6955–6964.
Haase H, Rink L (2014) Zinc signals and immune function. BioFactors 40:27–40.
Hellewell AL, Adams JC (2015) Insider trading: extracellular matrix proteins and their non-canonical intracellular roles. BioEssays 38:77–88.
Hidalgo J, Campmany L, Marti O, Armario A (1991) Metallothionein-I induction by stress in specific brain areas. Neurochem Res 16:1145–1148.
Hou P, Troen T, Ovejero MC, Kirkegaard T, Andersen TL, Byrjalsen I, Ferreras M, Sato T, Shapiro SD, Foged NT, Delaisse JM (2004) Matrix metalloproteinase-12 (MMP-12) in osteoclasts: new lesson on the involvement of MMPs in bone resorption. Bone 34:37–47.
Huber L, Brock M, Hemmatazad H, Giger O, Moritz F, Trenkmann M, Distler H, Gay R, Kolling C, Moch H, Michel B, Gay S, Distler O, Jüngel A (2007) Histone deacetylase/acetylase activity in total synovial tissue derived from rheumatoid arthritis and osteoarthritis patients. Arthritis Rheum 56:1087–1093.
Hur EM, Youssef S, Haws ME, Zhang SY, Sobel RA, Steinman L (2007) Osteopontin-induced relapse and progression of autoimmune brain disease through enhanced survival of activated T cells. Nat Immunol 8:74–83.
Iczkiewicz J, Jackson MJ, Smith LA, Rose S, Jenner P (2006) Osteopontin expression in substantia nigra in MPTP-treated primates and in Parkinson's disease. Brain Res 1118:239–250.
Iczkiewicz J, Broom L, Cooper JD, Wong AM, Rose S, Jenner P (2010) The RGD-containing peptide fragment of osteopontin protects tyrosine hydroxylase positive cells against toxic insult in primary ventral mesencephalic cultures and in the rat substantia nigra. J Neurochem 114:1792–1804.
Inoue M, Shinohara ML (2011) Intracellular osteopontin (iOPN) and immunity. Immunol Res 49:160–172.
Inoue K, Takano H, Shimada A, Satoh M (2009) Metallothionein as an anti-inflammatory mediator. Mediators Inflamm 2009:101659.
Isani G, Carpene E (2014) Metallothioneins, unconventional proteins from unconventional animals: a long journey from nematodes to mammals. Biomolecules 4:435–457.
Jakovac H, Grebic D, Tota M, Barac-Latas V, Mrakovcic-Sutic I, Milin C, Radosevic-Stasic B (2011) Time-course expression of metallothioneins and tissue metals in chronic relapsing form of experimental autoimmune encephalomyelitis. Histol Histopathol 26:233–245.
Jansson M, Panoutsakopoulou V, Baker J, Klein L, Cantor H (2002) Attenuated experimental autoimmune encephalomyelitis in Eta-1/osteopontin-deficient mice. J Immunol 168:2096–2099.
Kahles F, Findeisen HM, Bruemmer D (2014) Osteopontin: a novel regulator at the cross roads of inflammation, obesity and diabetes. Mol Metabol 3:384–393.
Kang W-S, Choi J-S, Shin Y-J, Kim H-Y, Cha J-H, Lee J-Y, Chun M-H, Lee M-Y (2008) Differential regulation of osteopontin receptors, CD44 and the αv and β3 integrin subunits, in the rat hippocampus following transient forebrain ischemia. Brain Res 1228:208–216.
Kazanecki CC, Uzwiak DJ, Denhardt DT (2007) Control of osteopontin signaling and function by post-translational phosphorylation and protein folding. J Cell Biochem 102:912–924.
Kim MD, Cho HJ, Shin T (2004) Expression of osteopontin and its ligand, CD44, in the spinal cords of Lewis rats with experimental autoimmune encephalomyelitis. J Neuroimmunol 151:78–84.
Ling X-B, Wei H-W, Wang J, Kong Y-Q, Wu Y-Y, Guo J-L, Li T-F, Li J-K (2016) Mammalian metallothionein-2A and oxidative stress. Int J Mol Sci 17:1483.
Lynes MA, Zaffuto K, Unfricht DW, Marusov G, Samson JS, Yin X (2006) The physiological roles of extracellular metallothionein. Exp Biol Med (Maywood) 231:1548–1554.
Manso Y, Adlard PA, Carrasco J, Vasak M, Hidalgo J (2011) Metallothionein and brain inflammation. J Biol Inorg Chem 16:1103–1113.
Miles AT, Hawksworth GM, Beattie JH, Rodilla V (2000) Induction, regulation, degradation, and biological significance of mammalian metallothioneins. Crit Rev Biochem Mol Biol 35:35–70.
Mocchegiani E, Muzzioli M, Giacconi R (2000) Zinc, metallothioneins, immune responses, survival and ageing. Biogerontology 1:133–143.
Morimoto J, Kon S, Matsui Y, Uede T (2010) Osteopontin; as a target molecule for the treatment of inflammatory diseases. Curr Drug Targets 11:494–505.
Morisaki Y, Niikura M, Watanabe M, Onishi K, Tanabe S, Moriwaki Y, Okuda T, Ohara S, Murayama S, Takao M, Uchida S, Yamanaka K, Misawa H (2016) Selective expression of osteopontin in ALS-resistant motor neurons is a critical determinant of late phase neurodegeneration mediated by matrix metalloproteinase-9. Sci Rep 6:27354.
Murugaiyan G, Mittal A, Weiner HL (2008) Increased osteopontin expression in dendritic cells amplifies IL-17 production by CD4 + T cells in experimental autoimmune encephalomyelitis and in multiple sclerosis. J Immunol 181:7480–7488.
Niino M, Kikuchi S (2011) Osteopontin and multiple sclerosis: an update. Clin Exp Neuroimmunol 2:33–40.
Okamoto H (2007) Osteopontin and cardiovascular system. Mol Cell Biochem 300:1–7.
O'Regan AW, Nau GJ, Chupp GL, Berman JS (2000) Osteopontin (Eta-1) in cell-mediated immunity: teaching an old dog new tricks. Immunol Today 21:475–478.
Pedersen MO, Jensen R, Pedersen DS, Skjolding AD, Hempel C, Maretty L, Penkowa M (2009) Metallothionein-I + II in neuroprotection. BioFactors 35:315–325.
Penkowa M (2006) Metallothioneins are multipurpose neuroprotectants during brain pathology. FEBS J 273:1857–1870.
Penkowa M, Hidalgo J (2003) Treatment with metallothionein prevents demyelination and axonal damage and increases oligodendrocyte precursors and tissue repair during experimental autoimmune encephalomyelitis. J Neurosci Res 72:574–586.
Penkowa M, Espejo C, Ortega-Aznar A, Hidalgo J, Montalban X, Martinez Caceres EM (2003) Metallothionein expression in the

central nervous system of multiple sclerosis patients. Cell Mol Life Sci 60:1258–1266.
Plantman S (2012) Osteopontin is upregulated after mechanical brain injury and stimulates neurite growth from hippocampal neurons through beta1 integrin and CD44. NeuroReport 23:647–652.
Plantman S (2013) Proregenerative properties of ECM molecules. Biomed Res Int 2013:981695.
Prasad AS (2008) Clinical, immunological, anti-inflammatory and antioxidant roles of zinc. Exp Gerontol 43:370–377.
Rink L, Haase H (2007) Zinc homeostasis and immunity. Trends Immunol 28:1–4.
Rittling SR, Singh R (2015) Osteopontin in immune-mediated diseases. J Dent Res 94:1638–1645.
Scatena M, Liaw L, Giachelli CM (2007) Osteopontin: a multifunctional molecule regulating chronic inflammation and vascular disease. Arterioscler Thromb Vasc Biol 27:2302–2309.
Selvaraju R, Bernasconi L, Losberger C, Graber P, Kadi L, Avellana-Adalid V, Picard-Riera N, Van Evercooren AB, Cirillo R, Kosco-Vilbois M, Feger G, Papoian R, Boschert U (2004) Osteopontin is upregulated during in vivo demyelination and remyelination and enhances myelin formation in vitro. Mol Cell Neurosci 25:707–721.
Senger DR, Wirth DF, Hynes RO (1979) Transformed mammalian cells secrete specific proteins and phosphoproteins. Cell 16:885–893.
Sharma S, Rais A, Sandhu R, Nel W, Ebadi M (2013) Clinical significance of metallothioneins in cell therapy and nanomedicine. Int J Nanomed 8:1477–1488.
Shinohara ML, Kim JH, Garcia VA, Cantor H (2008a) Engagement of the type-I interferon receptor on dendritic cells inhibits promotion of Th17 cells: role of intracellular osteopontin. Immunity 29:68–78.
Shinohara ML, Kim HJ, Kim JH, Garcia VA, Cantor H (2008b) Alternative translation of osteopontin generates intracellular and secreted isoforms that mediate distinct biological activities in dendritic cells. Proc Natl Acad Sci U S A 105:7235–7239.
Smith LL, Cheung HK, Ling LE, Chen J, Sheppard D, Pytela R, Giachelli CM (1996) Osteopontin N-terminal domain contains a cryptic adhesive sequence recognized by alpha9beta1 integrin. J Biol Chem 28485–28491.
Steinman L (2009) A molecular trio in relapse and remission in multiple sclerosis. Nat Rev Immunol 9:440–447.
Subraman V, Thiyagarajan M, Malathi N, Rajan ST (2015) OPN - revisited. J Clin Diagn Res 9:ZE10–ZE13.
Teramoto H, Castellone MD, Malek RL, Letwin N, Frank B, Gutkind JS, Lee NH (2004) Autocrine activation of an osteopontin-CD44-Rac pathway enhances invasion and transformation by H-RasV12. Oncogene 24:489–501.
Weber GF, Ashkar S, Glimcher MJ, Cantor H (1999) Receptor-ligand interaction, between CD44 and osteopontin (Eta-1). Science 271:509–512.
Wright MC, Mi R, Connor E, Reed N, Vyas A, Alspalter M, Coppola G, Geschwind DH, Brushart TM, Hoke A (2014) Novel roles for osteopontin and clusterin in peripheral motor and sensory axon regeneration. J Neurosci 34:1689–1700.
Wu X, Reddy DS (2012) Integrins as receptor targets for neurological disorders. Pharmacol Ther 134:68–81.
Yokosaki Y, Matsuura N, Sasaki T, Murakami I, Schneider H, Higashiyama S, Saitoh Y, Yamakido M, Taooka Y, Sheppard D (1999) The integrin alpha(9)beta(1) binds to a novel recognition sequence (SVVYGLR) in the thrombin-cleaved amino-terminal fragment of osteopontin. J Biol Chem 274:36328–36334.
Yokosaki Y, Tanaka K, Higashikawa F, Yamashita K, Eboshida A (2005) Distinct structural requirements for binding of the integrins alphavbeta6, alphavbeta3, alphavbeta5, alpha5beta1 and alpha9beta1 to osteopontin. Matrix Biol 24:418–427.
Zhao C, Fancy SP, ffrench-Constant C, Franklin RJ (2008) Osteopontin is extensively expressed by macrophages following CNS demyelination but has a redundant role in remyelination. Neurobiol Dis 31:209–217.

(Received 20 December 2016, Accepted 14 March 2017)
(Available online 24 March 2017)